

End-to-End Asynchronous Traffic Scheduling in Converged 5G and Time-Sensitive Networks

Jiacheng Li, Yongxiang Zhao, Chunxi Li, Zonghui Li, Kang G. Shin, *Life Fellow, IEEE*, and Bo Ai, *Fellow, IEEE*

Abstract—As required by Industry 4.0, companies will move towards flexible and individual manufacturing. To succeed in this transition, convergence of 5G and time-sensitive networks (TSN) is the most promising technology and has thus attracted considerable interest from industry and standardization groups. However, the delay and jitter of end-to-end (e2e) transmission will get exacerbated if the transmission opportunities are missed in TSN due to the 5G transmission jitter and the clock skew between the two network systems. To mitigate this phenomenon, we propose a novel asynchronous access mechanism (AAM) that isolates the jitter only in the 5G system and ensures zero transmission jitter in TSN. We then exploit AAM to develop an e2e asynchronous traffic scheduling model for coordinated allocation of resources for 5G and TSN to provide e2e transmission delay guarantees for time-critical flows. The results of our extensive simulation of AAM on OMNET++ corroborate the superior performance of AAM and the scheduling model.

Index Terms—end-to-end(e2e), traffic scheduling, asynchronous access, deterministic transmission, jitter isolation, TSN, 5G.

I. INTRODUCTION

MORE and more industrial use-cases require low-delay communication to enable production automation [1], [2], such as the control of cooperating robots [3] and Automated Guided Vehicles (AGVs) [4]. Real-time networks serve as the foundation for providing deterministic and reliable transmission for such industrial time-sensitive communication. According to the prevalent transmission media, industrial real-time networks can be characterized as a combination of wired and wireless networks.

Current industrial real-time networks are still dominated by wired technologies [5] such as CAN, PROFIBUS, EtherCAT, and TTEthernet. However, these technologies either have low data-rate [6], or are manufacturer-specific, thereby making them incompatible with each other [7]. Consequently, IEEE 802.1 Time-Sensitive Networking (TSN) [8], which defines a variety of mechanisms such as time synchronization and traffic shaping to guarantee deterministic transmission, has been a

promising solution for future unified industrial networks in the wired environment [9].

However, such a wired technology is only suitable for production facilities that are static and have long life cycles [10], thus lacking the flexibility and modularity [11], [12] required by Industry 4.0. The industry and academia, therefore, turn to wireless technology to achieve this goal [10], [13].

The fifth-generation cellular network technology (5G), which considered industrial use-cases from the very beginning, has been considered as a key technology for two reasons. First, its ultra-reliable low-delay communication (URLLC) feature provides a flexible frame structure, faster signaling, etc., to support low-delay communication [14]. Second, 3GPP has completed the integration architecture of 5G system (5GS) and TSN [15], which includes additional functionalities, such as the Network-side TSN translator (NW-TT) for user plane function (UPF) to access TSN.

However, simple integration of 5GS and TSN may significantly exacerbate the delay and jitter in packet delivery. First, assuming TSN uses the time-aware shaper (TAS), each packet from 5GS must arrive at the gateway before the start of its "prepared" transmission opportunity in TSN, which we call the *time-triggered access mechanism* (TAM). Second, it is difficult for 5GS to successfully deliver a packet before the start of its transmission opportunity owing to (1) the transmission jitter caused by wireless transmission in 5GS and (2) the clock skew between 5GS and TSN. Thus, if a packet output by 5GS misses its transmission opportunity in TSN, it has to wait for the opportunity assigned to the next packet. Since the interval between TSN transmission opportunities is much larger than (1) and (2), missing a transmission opportunity will enlarge the e2e delay and jitter significantly.

To mitigate this delay and jitter enlargement, we propose a novel *asynchronous access mechanism* (AAM) to bridge 5GS and TSN. By decoupling the transmission interaction between 5GS and TSN, the AAM ensures zero transmission jitter in TSN at the cost of the wired transmission bandwidth, no matter how randomly the packets arrive at TSN from 5GS. Using the AAM, we then build an e2e *asynchronous traffic scheduling model* (ATSM) to allocate the resources of TSN and 5GS. We then validate the performance of AAM and ATSM via simulation on OMNET++ [16].

The remainder of this paper is organized as follows. Section II discusses the related work while Section III introduces the delay and jitter enlargement in the context of TAM and mitigates it with the AAM. Section IV proposes the ATSM based on the AAM. Section V evaluates the performance of the AAM and the ATSM. Finally, this paper concludes with

Manuscript received ; revised . This work was supported in part by the National Key Research and Development Project under Grant 2022YFB3303702, and in part by the National Natural Science Foundation of China under Grant 62002013 and Grant 62272034. (*Corresponding author: Zonghui Li*)

Jiacheng Li, Yongxiang Zhao, Chunxi Li and Bo Ai are with the School of Electronic and Information Engineering, Beijing Jiaotong University, Beijing 100044, China (e-mail: 21120075@bjtu.edu.cn; yxzhao@bjtu.edu.cn; chxli1@bjtu.edu.cn; boai@bjtu.edu.cn).

Zonghui Li is with the School of Computer and Information Technology, Beijing Jiaotong University, Beijing 100044, China (e-mail: li-zonghui@bjtu.edu.cn).

Kang G. Shin is with the Department of Electrical Engineering and Computer Science, University of Michigan, Ann Arbor, MI 48109-2121, USA (e-mail: kgshin@umich.edu).

Section VI.

II. RELATED WORK

The traffic scheduling for the converged network of 5G and TSN is still in its infancy and can be treated as either separate or joint scheduling depending on whether the resources in the two networks are allocated cooperatively or not.

In the case of separate scheduling, the e2e delay requirement of a time-critical flow is first divided into 5GS and TSN delay budgets, and then the two networks schedule their own network resources independently according to their own delay budget. [17] scheduled multiple resource blocks (RBs) for multiple packets of time-critical flows to solve the periodic resource conflict in 5GS. [18] dynamically mapped the QoS requirements obtained from time-sensitive communication assistance information (TSCAI) to 5G QoS Identifier (5QI), and added dynamic RBs to pre-allocated RBs if the latter was insufficient for data transmission. [19] maximized the ratio of eMBB traffic throughput to URLLC traffic delay given the flow information from TSCAI. Most of the related work was devoted to studying how to achieve the resource allocation in 5GS given the 5GS delay budget without considering how to allocate delay budgets to TSN and 5GS.

Joint scheduling manages the use of resources cooperatively in TSN and 5GS from an e2e perspective. The authors of [20] proposed a unified scheduling model to allocate appropriate time slots for time-critical flows using the cyclic queuing and forwarding (CQF) mechanism and proposed a reinforcement learning-based algorithm to search for the optimal scheduling solution. [21] maintained the freshness of information by scheduling sampling and transmission decisions cooperatively to reduce energy consumption. The flow pattern output from TSN to 5GS was found in [11] to have a significant impact on the capacity and delay in 5GS, and [22] proposed an e2e-optimized scheduling framework to jointly schedule the resources of the two network systems. All these works assumed that 5GS and TSN were synchronized.

However, we find the transmission interaction between 5GS and TSN possibly resulting in the delay and jitter enlargement as mentioned in Section I. To mitigate this, we propose the AAM, which enables the converged network to run in asynchronous conditions. Furthermore, we propose the ATSM based on the AAM to coordinate the allocation of 5GS and TSN resources.

III. ASYNCHRONOUS ACCESS MECHANISM

We first introduce the application scenario and the e2e delay and jitter enlargement in the context of TAM. The basic ideas and implementation details of AAM are then presented to mitigate this problem.

A. Application Scenario

Fig. 1 shows an application scenario in which a TSN and a 5GS are connected via a gateway (GW). TSN is composed of end-stations (ESs) and TSN switches while 5GS is composed of user equipment (UEs) and a base station (BS). All the flows under consideration originate from UEs in 5GS to the ESs in

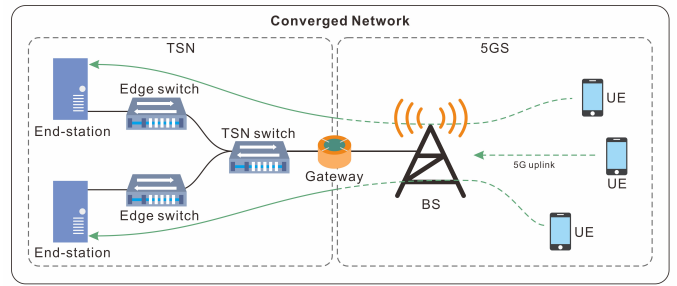


Fig. 1. The converged network that integrates 5GS and TSN.

TSN and belong to time-triggered (TT) flows. Specifically, the source of a TT flow periodically generates fixed-length packets. Each TT flow is subject to the e2e delay requirement for packet delivery.

Additionally, we assume that the clocks in TSN and 5GS are synchronous within their respective domains but can be asynchronous between different domains. Each TSN switch adopts TAS on each port. We also assume that 5GS uses the FDD duplex scheme where downlink and uplink transmissions use different frequencies and all UEs share a common 5G uplink.

B. Delay and Jitter Enlargement

Using an example, we show below that the simple integration of 5GS and TSN may enlarge e2e delay and jitter, where the simple integration means TAS’s reservation of a transmission opportunity for each frame of a TT flow on each link on its route.

In Figs. 2a–2d, the UE in 5GS sends a packet every 100ms to the ES in TSN via the GW and edge switch (Edge). We will use Figs. 2a and 2b to show the enlargement of delay and jitter caused by the clock skew between 5GS and TSN and the 5G transmission jitter, respectively.

As shown in Fig. 2a, in an ideal situation — i.e., there is no 5G transmission jitter or clock skew between 5GS and TSN — GW and Edge reserve a transmission opportunity every 100ms (= the flow period) on their output port, which is shown as black hollow circles, and the black dashed arrows depict the ideal transmission processes. Each packet experiences a constant delay of 45ms and the e2e jitter of 0. However, considering the clock skew between the two systems, the packets may arrive at TSN earlier (depicted by the blue line) or later (depicted by the red line) from the perspective of TSN. We assume the maximum clock skew is 10ms, i.e., the clock of TSN may be at most 10ms earlier or later than that of 5GS. On the one hand, packet #1 arrives 10ms earlier than the prepared transmission opportunity and has to wait for it, leading to the actual e2e delay of 55ms. On the other hand, packet #2 arrives 10ms later than the prepared transmission opportunity and must wait for the opportunity in the next period, leading to the actual e2e delay of 135ms. Actually, the experienced e2e delay can be as low as 45ms and as large as 145ms, creating a deviation of 100ms which equals the flow period. Thus, a small skew between the clocks of the

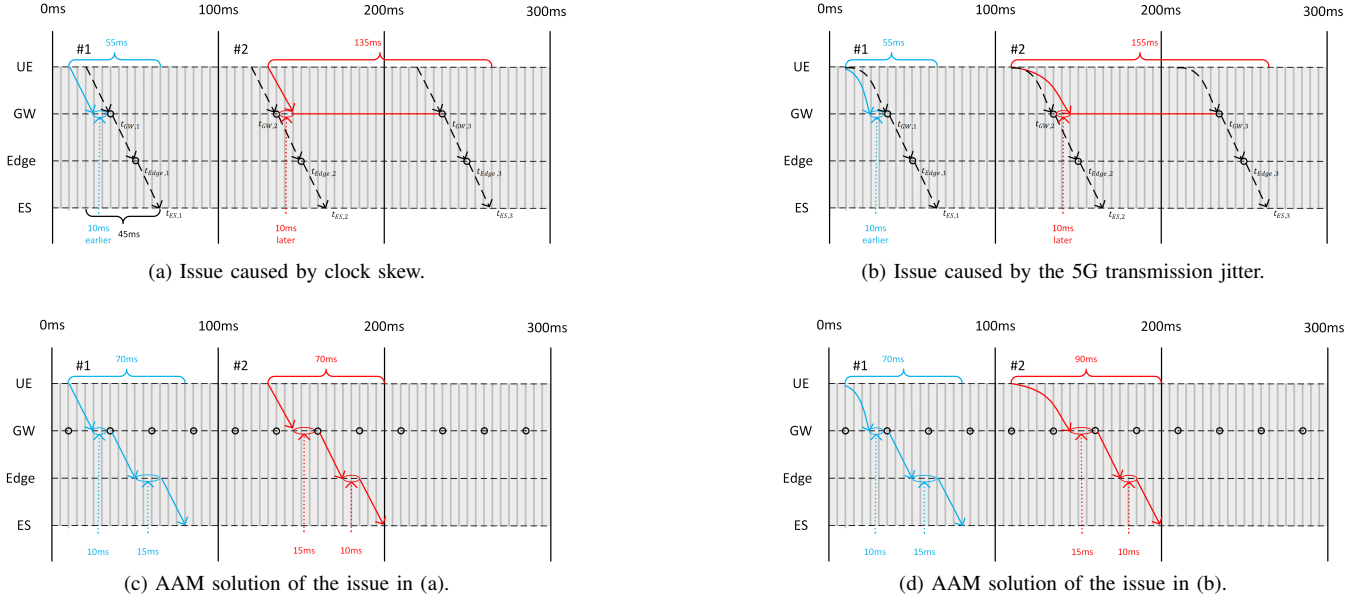


Fig. 2. Issues caused by the 5G transmission jitter and the clock skew in the context of TAM and their mitigation with AAM.

two systems may lead to a significantly larger e2e delay and jitter than scheduled.

Similarly, as shown in Fig. 2b, we assume that the clocks are synchronized, the delay budget in 5GS is estimated to be the average delay over a period of time, and the transmission opportunities prepared by TSN are scheduled by reserving the delay budget of 5GS. The transmission jitter of 5GS is 10ms, meaning packets may arrive at most 10ms quicker or slower than the ideal arrival time calculated by the delay budget. Packet #1 experiences an e2e delay of 55ms while packet #2 experiences 155ms and their deviation shown in the figure is thus 100ms, which also equals the flow period. A small 5G transmission jitter may also lead to a significantly larger e2e delay and jitter than scheduled.

In fact, the e2e delay and jitter enlargement is caused by missing TSN transmission opportunities. To mitigate this enlargement, we propose the AAM to decouple the interaction between 5GS and TSN transmissions.

C. Basic Ideas of the AAM

The basic ideas of the AAM are to (1) hold the packets at the edge switches to shape the resident time in TSN to be constant and (2) over-provision the transmission opportunities to reduce delay.

First, a holding process is introduced in the edge switch. Let T_i be the period of the transmission opportunities (not necessarily equals the flow period as will be discussed later). As shown in Fig. 2c, $T_i = 25ms$. Packets #1 and #2 experience similar transmission processes: (1) waiting at the GW, (2) transmitted from GW to Edge, (3) held at the Edge, and (4) transmitted from Edge to ES, and the corresponding delays are denoted as $f_i.wait$, $D_{i,(1)}^{TSN}$, $f_i.hold$ and $D_{i,(2)}^{TSN}$. The delay in TSN can be represented as:

$$D_i^{TSN} = f_i.wait + D_{i,(1)}^{TSN} + f_i.hold + D_{i,(2)}^{TSN}, \quad (1)$$

where $D_{i,(1)}^{TSN}$ and $D_{i,(2)}^{TSN}$ are both constant assuming TSN is well organized. It is easy to get $f_i.wait \in [0, T_i)$ so the holding time is for compensating the waiting time to be T_i , i.e., $f_i.wait + f_i.hold = T_i$. As can be seen from Fig. 2c, packet #1 waits for 10ms and is held for 15ms, and packet #2 waits for 15ms and is held only for 10ms. This way, the packets' resident time in TSN is fixed and can be represented as:

$$D_i^{TSN} = T_i + D_{i,(1)}^{TSN} + D_{i,(2)}^{TSN}. \quad (2)$$

So, all the packets of the flow experience the same delay in TSN no matter when the packets are delivered by 5GS, and the transmission coupling between the two network systems is eliminated, hence mitigating the delay and jitter enlargement. As shown in Fig. 2c, both packets experience the same e2e delay of 70ms regardless of the clock skew between the two network systems.

However, in many industrial use-cases [6] the delay requirement is no larger than the period. If $T_i = f_i.period$, the delay requirement cannot be satisfied according to Eq. (2). This way the transmission opportunities are over-provisioned to reduce delay, i.e., T_i should be less than $f_i.period$.

Similarly, Fig. 2d illustrates how the AAM can help mitigate the issues presented in Fig. 2b. Moreover, the e2e transmission jitter is isolated only in 5GS.

Note that the parameter T_i should be carefully determined to balance between the resource usage and the delay in TSN, and between the delay budgets in TSN and 5GS for the following reasons:

- T_i allows for a trade-off between usage of TSN resource and the delay in TSN. According to Eq. (2), the smaller T_i , the lower the delay in TSN. However, a smaller T_i means more TSN resource usage for a single flow as shown in Figs. 2a and 2c.

- T_i balances the delay budgets in 5GS and TSN. The e2e delay is composed of 5G and TSN parts:

$$\begin{aligned} D_i^{e2e} &= D_i^{5GS} + D_i^{TSN} \\ &= D_i^{5GS} + T_i + D_{i,(1)}^{TSN} + D_{i,(2)}^{TSN}. \end{aligned} \quad (3)$$

Given the e2e delay requirement of a flow, a larger T_i will decrease the delay budget allocated to 5GS which will affect the performance of 5GS.

It is, therefore, necessary to establish a comprehensive model to jointly schedule the resources of 5GS and TSN when the AAM is applied; this will be discussed in Section IV.

D. Implementation of the AAM

The AAM is composed of the following two parts.

- The gateway caches the received packet of f_i until the next transmission opportunity, attaches the waiting time $f_i.wait$ and sends it to the destination.
- The edge switch of the last hop holds the packet of f_i for time duration $f_i.hold$ and then delivers it to the final destination, where $f_i.hold + f_i.wait = T_i$.

The implementation details in the gateway and the edge switch are described in Algorithms 1 and 2, respectively.

Algorithm 1: AAM at the gateway

```

1 function onReceivingPacketFrom5GS( $f_i.packet$ ):
2    $f_i.buffer = f_i.packet.getPayload()$ ;
3    $f_i.receivedTime = now()$ ;
4 function onTransmissionOpportunity( $f_i.timer$ ):
5    $resetTimer(f_i.timer)$ ;
6   if  $f_i.buffer$  is empty then
7     return;
8   else
9      $new\ f_i.packet$ ;
10     $f_i.packet.setPayload(f_i.buffer)$ ;
11     $f_i.packet.setWait(now() - f_i.receivedTime)$ ;
12     $send(f_i.packet)$ ;
13     $f_i.buffer.reset()$ ;
14  end
    
```

Algorithm 2: AAM at the edge switch

```

1 function onReceivingPacket( $f_i.packet$ ):
2    $delay(f_i.T - f_i.packet.getWait())$ ;
3    $send(f_i.packet)$ ;
    
```

In Algorithm 1, there are two functions in the gateway. In the first function $onReceivingPacketFrom5GS(f_i.packet)$, once the packet of flow f_i is received, the gateway caches the packet in the buffer $f_i.buffer$ prepared for this flow (Line 2). If there is already a packet in the buffer, the old packet will be replaced by the new packet. Then, the reception time of the packet is recorded (Line 3). In the second function $onTransmissionOpportunity(f_i.timer)$, the function takes a timer as an input parameter. Since a timer is set for each flow f_i to inform its transmission, the function first resets the timer

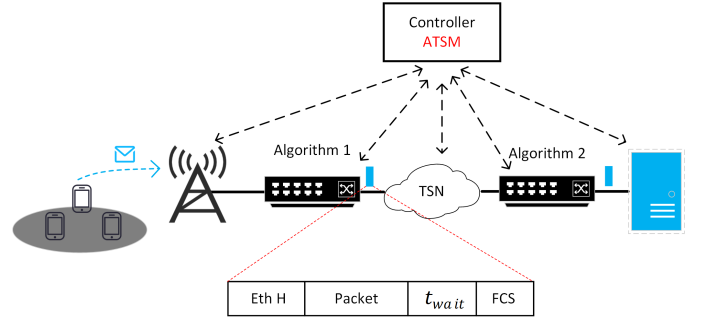


Fig. 3. An example of the deployment of the AAM.

for the next transmission opportunity for this flow (Line 5). It then checks whether the buffer of this flow is empty. On the one hand, the function does nothing if the corresponding buffer is empty. On the other hand, it attaches the waiting time to this packet and sends it before clearing the buffer if the buffer is not empty (Lines 6-13).

There is only one function in Algorithm 2. When the edge switch receives the packet $f_i.packet$, it delays the packet for the amount of time $f_i.T - f_i.packet.getWait()$ which is consistent with the process mentioned before (Line 2). The packet is then delivered to the destination after the delay (Line 3).

As shown in Fig. 3, AAM can be easily integrated into the 5GS-TSN architecture proposed in [15]. The base station complies with the 5G Network standard. The two black boxes implement Algorithm 1 and 2, respectively, and they are connected by a traditional TSN network. The frame's waiting time at the left black box is incorporated into the frame payload and the right black box can extract the time from the received frames. The ATSM is implemented in the controller, whose detailed structure can be found from [15]. The controller collects the state of the converged network and flows' requirements, and then calculates the settings of 5GS, TSN, and the two black boxes.

IV. ASYNCHRONOUS TRAFFIC SCHEDULING MODEL

We now formally present ATSM to schedule the resources in the converged network based on AAM. The network and traffic models are introduced first and the scheduling model is presented to formulate the scheduling problem. We then derive the formal network constraints and the objective function. Finally, a linearization method is introduced to transform the scheduling problem to an Integer Linear Programming problem.

A. Network and Traffic Models

The wired TSN network is defined as an undirected graph $G(V, E)$, where V is the set of nodes such as ESs, the gateway, and TSN switches, and E is the set of physical full-duplex links in TSN. Specifically, each physical link contains two dataflow links [23]. Let L^{TSN} denote the set of dataflow links in TSN, then

$$\forall v_1, v_2 \in V, (v_1, v_2) \in E : [v_1, v_2], [v_2, v_1] \in L^{TSN}, \quad (4)$$

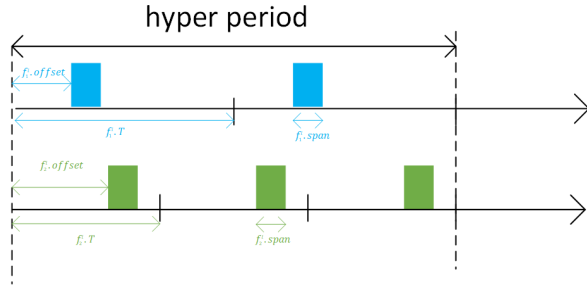


Fig. 4. Scheduling example in TSN.

where “ (v_1, v_2) ” denotes the physical link between nodes v_1 and v_2 , “ $[v_1, v_2]$ ” and “ $[v_2, v_1]$ ” are the corresponding directed dataflow links.

The set of dataflow links in 5GS is denoted as L^{5GS} . The entire set of dataflow links in the converged network can then be represented as $L = \{L^{TSN}, L^{5GS}\}$.

Let F be the set flows under consideration. Each flow $f_i \in F$ is identified as:

$$\forall f_i \in F : \langle f_i.period, f_i.length, f_i.delay \rangle, \quad (5)$$

where $f_i.period$ denotes the period of the flow, $f_i.length$ the packet length of the flow in one period, and $f_i.delay$ the e2e delay boundary required by the flow.

For each flow, we assume there is only one frame to be delivered within one period, and the route is determined in advance:

$$\forall f_i \in F : p_i = [l_1, l_2, \dots, l_{h_i}], l_j \in L, \quad (6)$$

where h_i is the number of hops for f_i . Table I summarizes the main notations/symbols used in this paper.

B. Scheduling Model

We formally define the transmission opportunities reserved in TSN and 5GS as potential transmission instances.¹ Let f_i^l denote the potential transmission instance of flow f_i on the dataflow link l .

1) *Scheduling model in TSN*: In TSN, the potential transmission instance f_i^l is fully determined by the following triple:

$$\forall f_i \in F, \forall l \in p_i \cap L^{TSN} : \\ f_i^l = \{f_i^l.T, f_i^l.offset, f_i^l.span\} \quad (7)$$

where $f_i^l.T$ denotes the period of the transmission opportunities reserved for f_i on the dataflow link l , while $f_i^l.offset$ and $f_i^l.span$ denote the offset and the transmission duration. Fig. 4 shows an example.

For a single flow, $f_i^l.T$ is the same along its route (denoted as T_i) and $f_i^l.span$ is the ratio of the frame length to the link rate which is known *a priori*, and the pattern repeats in

¹Since each transmission opportunity is allocated to an actually transmitted packet in the traditional traffic scheduling model of TSN, each transmission opportunity is also called a *transmission instance* [24]. However, in the AAM context, not every transmission opportunity corresponds to an actually transmitted packet. So, we extend the concept of transmission instances to potential transmission instances.

 TABLE I
 NOTATIONS USED IN THIS WORK.

Symbol	Description
G	the wired TSN network
V	the set of nodes in TSN
E	the set of wired links in TSN
F	the set of all flows
L, L^{TSN}, L^{5GS}	the set of dataflow links of the whole network, TSN, and 5GS
$v_i \in V$	the node of TSN
$(v_1, v_2) \in E$	the physical link between nodes v_1 and v_2
$[v_1, v_2], [v_2, v_1] \in L^{TSN}$	the dataflow links between nodes v_1 and v_2
$f_i \in F$	one flow of the set F
p_i	the route of flow f_i
h_i	the number of hops of the route p_i
T_i	the period of transmission opportunities reserved in TSN for f_i
$f_i.period, f_i.length, f_i.delay$	the period, length, and delay requirement of f_i
f_i^l	the potential transmission instance of f_i on dataflow link l
$f_i^l.T, f_i^l.offset, f_i^l.span$	the transmission period, start offset, and transmission delay of the f_i^l
\mathcal{F}	the whole set of RBs in 5GS
k, k_{max}	the k^{th} RB and the whole number of RBs
$x_{i,k}^l$	whether the k^{th} RB of dataflow link l is assigned to f_i
y_k^l	whether the k^{th} RB of dataflow link l is assigned to any flow
$minP$	the minimum period supported by TSN
T_{TSN}	the TSN hyper period
T_{5GS}	the 5GS hyper period

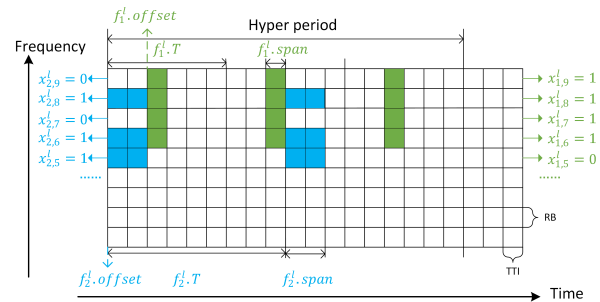


Fig. 5. Scheduling example in 5GS.

every cycle. For multiple flows, the pattern similarly repeats in every “hyper period”. TSN’s hyper period is defined as the least common multiple of the periods of every flow’s potential transmission instances:

$$T_{TSN} = LCM(\{T_i | f_i \in F\}). \quad (8)$$

As shown in Fig. 4, the reference zero points of all potential transmission instances of all flows are the same, and in one hyper period, the potential transmission instance of f_1 on dataflow link l appears twice while that of f_2 appears thrice.

The values of $f_i^l.T$ and $f_i^l.offset$ for all flows $f_i \in F$ on TSN dataflow links of its route $l \in p_i \cap L^{TSN}$ (except for the last dataflow link) are design variables.

2) *Scheduling model in 5GS*: As shown in Fig. 5, the resources in 5GS can be split into two dimensions: transmission

time intervals (TTI) in the time domain and the resource blocks (RBs) in the frequency domain.

Assuming there can be at most k_{max} RBs being allocated to these flows, the set of RBs is denoted as $\mathcal{F} = \{1, 2, \dots, k_{max}\}$. In 5GS, we use the SPS that reserves periodic resources for transmission [25]. To reduce the scheduling complexity, one potential transmission instance in 5GS can only occupy consecutive TTIs but we do not impose any constraint on the frequency domain. For example, as shown in Fig. 5, the potential transmission instances of f_2 occupy consecutive TTIs but non-consecutive RBs.

The potential transmission instance in 5GS can thus be identified by the following variables:

$$\forall f_i \in F, \forall l \in p_i \cap L^{5GS} : \\ f_i^l = \{f_i^l.T, f_i^l.offset, f_i^l.span, x_i^l\} \quad (9)$$

$$x_i^l = \{x_{i,k}^l | k \in \mathcal{F}\} \quad (10)$$

where $f_i^l.T$ is the flow's period and $x_{i,k}^l$ is a binary variable equal to 1 (0) if flow f_i is (not) allocated to RB k on dataflow link l . The variables $x_{i,k}^l$ allow us to schedule the RBs assigned to the flow while the variables $f_i^l.span$ are used to schedule the consecutive TTIs.

The concept of the hyper period also applies to 5GS:

$$T_{5GS} = LCM(\{f_i.period | f_i \in F\}). \quad (11)$$

The values of $f_i^l.offset$, $f_i^l.span$ and $x_{i,k}^l$ for all flows $f_i \in F$ on 5G dataflow links of its route $l \in p_i \cap L^{5GS}$ and each RB $k \in \mathcal{F}$ are design parameters.

C. Network Constraints

We now derive the constraints of the ATSM which accounts for both 5GS and TSN and schedules flows from an e2e perspective. The constraints introduced in IV-C6, IV-C7, IV-C8, and IV-C9 are borrowed from the mature scheduling model in TSN [6], [22], but are modified, if needed, for the AAM.

1) *Transmission-opportunity constraints*: Every packet in 5GS cannot start its transmission except for the start of TTI and the transmission time of a packet must be an integer multiple of TTI:

$$\forall l \in L^{5GS}, \forall f_i \in F : \\ \exists f_i^l \Rightarrow \\ f_i^l.offset = c_i^l \times TTI \quad (12)$$

$$f_i^l.span = d_i^l \times TTI \quad (13)$$

$$f_i^l.offset + f_i^l.span \leq f_i.period \quad (14)$$

$$c_i^l \in \{0, 1, \dots, \lfloor \frac{f_i.period}{TTI} \rfloor - 1\}$$

$$d_i^l \in \{1, 2, \dots, \lfloor \frac{f_i.period}{TTI} \rfloor\},$$

where c_i^l denotes the TTI flow f_i can start transmission in the 5G dataflow link l and d_i^l is the number of consecutive TTIs occupied by the flow on the allocated RBs.

2) *RB constraints*: We use binary variables y_k^l to indicate whether the k^{th} RB of 5G dataflow link l is scheduled to any flow. Specifically, $y_k^l = 1(0)$ if it is (not) assigned to any flow. So, we derive the following constraints:

$$\forall l \in L^{5GS}, \forall k \in \mathcal{F} : \\ \sum_{f_i \in F} x_{i,k}^l \leq y_k^l \times M, \quad (15)$$

where M is a (theoretically) infinitely large constant. The constraints guarantee that if $y_k^l = 0$, all $x_{i,k}^l$ for all flows should be 0.

3) *Resource constraints*: The resources allocated to a flow should be sufficient to transmit its packets. Let $R_{i,k}^l$ denote the number of bytes that can be transmitted by the k^{th} RB on the dataflow link l for the flow f_i which can be obtained from the simulator, then we have:

$$\forall l \in L^{5GS}, \forall f_i \in F : \\ \exists f_i^l \Rightarrow \\ \sum_{k=1}^{k_{max}} x_{i,k}^l \times R_{i,k}^l \times d_i^l \geq f_i.length \quad (16)$$

$$\sum_{k=1}^{k_{max}} x_{i,k}^l \times R_{i,k}^l \times (d_i^l - 1) < f_i.length \quad (17) \\ 1 \leq d_i^l \leq \lfloor \frac{f_i.period}{TTI} \rfloor$$

4) *OFDMA constraints*: Any two flows cannot be assigned to the same TTI on the same RB just as shown for f_1 and f_2 in Fig. 5:

$$\forall l \in L^{5GS}, \forall f_i, f_j \in F, \forall k \in \mathcal{F}, \\ \forall \alpha \in [0, (\frac{T_{5GS}}{f_i.period} - 1)], \\ \forall \beta \in [0, (\frac{T_{5GS}}{f_j.period} - 1)] : \\ ((f_i \neq f_j) \wedge \exists f_i^l \wedge \exists f_j^l) \Rightarrow \\ ((\alpha \times f_i.period) + f_i^l.offset + M \times (2 - x_{i,k}^l - x_{j,k}^l) \geq \\ (\beta \times f_j.period) + f_j^l.offset + f_j^l.span) \vee \\ ((\beta \times f_j.period) + f_j^l.offset + M \times (2 - x_{i,k}^l - x_{j,k}^l) \geq \\ (\alpha \times f_i.period) + f_i^l.offset + f_i^l.span). \quad (18)$$

5) *Window constraints*: Potential transmission instances have the same period along the route of the flow, and the period should not be larger than that of the flow. Therefore,

$$\forall l \in L^{TSN}, \forall f_i \in F : \\ (\exists f_i^l \wedge (l \neq l_{h_i})) \Rightarrow \\ f_i^l.T = T_i \quad (19)$$

$$f_i^l.T \leq f_i.period. \quad (20)$$

6) *Frame constraints*: The offset should be positive, and for simplicity a potential transmission instance should finish the transmission within its period:

$$\begin{aligned} \forall l \in L^{TSN}, \forall f_i \in F : \\ (\exists f_i^l \wedge (l \neq l_{h_i})) \Rightarrow \\ f_i^l.offset \geq 0 \end{aligned} \quad (21)$$

$$f_i^l.offset + f_i^l.span \leq T_i. \quad (22)$$

7) *Transmission order constraints*: The transmission opportunity on the next wired dataflow link l_b should send the packet after it is fully received over the preceding wired dataflow link l_a :

$$\begin{aligned} \forall l_a, l_b \in L^{TSN}, \forall f_i \in F : \\ (\exists f_i^{l_a} \wedge \exists f_i^{l_b} \wedge isNextHop(l_b, l_a, f_i) \wedge (l_b \neq l_{h_i})) \Rightarrow \\ f_i^{l_b}.offset \geq f_i^{l_a}.offset + f_i^{l_a}.span + ldelay^{l_a}, \end{aligned} \quad (23)$$

where $ldelay^{l_a}$ is the propagation delay of the dataflow link l_a and function $isNextHop(l_b, l_a, f_i)$ returns true if l_b is the next dataflow link of l_a on the route of flow f_i else false.

8) *TDMA constraints*: Wired links can only transmit one frame at a time, and hence potential transmission instances reserved for different flows should not overlap:

$$\begin{aligned} \forall l \in L^{TSN}, \forall f_i, f_j \in F, \\ \forall \alpha \in [0..(\frac{T_{TSN}}{T_i} - 1)], \\ \forall \beta \in [0..(\frac{T_{TSN}}{T_j} - 1)] : \\ ((f_i \neq f_j) \wedge \exists f_i^l \wedge \exists f_j^l \wedge (l \neq l_{h_i}) \wedge (l \neq l_{h_j})) \Rightarrow \\ ((\alpha \times T_i) + f_i^l.offset \geq \\ (\beta \times T_j) + f_j^l.offset + f_j^l.span) \vee \\ ((\beta \times T_j) + f_j^l.offset \geq \\ (\alpha \times T_i) + f_i^l.offset + f_i^l.span). \end{aligned} \quad (24)$$

Note that the T_{TSN} contains the scheduling parameters while it is fixed in the traditional scheduling of TSN. We will discuss how to linearize these constraints in Section IV-E.

9) *Frame isolation constraints*: If frames of different flows arrive at the same TSN switch at the same time and have the same output port, the order that the frames in the queue is not certain hence introducing non-determinism [6]. So, only frames from the same flow can be stored in the queue:

$$\begin{aligned} \forall l_a, l_b, l_c \in L^{TSN}, \forall f_i, f_j \in F, \\ \forall \alpha \in [0..(\frac{T_{TSN}}{T_i} - 1)], \\ \forall \beta \in [0..(\frac{T_{TSN}}{T_j} - 1)] : \\ ((f_i \neq f_j) \wedge \\ \exists f_i^{l_a} \wedge \exists f_i^{l_c} \wedge \exists f_j^{l_b} \wedge \exists f_j^{l_c} \wedge \\ isNextHop(l_c, l_a, f_i) \wedge \\ isNextHop(l_c, l_b, f_j) \wedge \\ (l_c \neq l_{h_i}) \wedge (l_c \neq l_{h_j})) \Rightarrow \\ (((\alpha \times T_i) + f_i^{l_c}.offset \leq \end{aligned}$$

$$\begin{aligned} (\beta \times T_j) + f_j^{l_b}.offset + ldelay^{l_b}) \vee \\ ((\beta \times T_j) + f_j^{l_c}.offset \leq \\ (\alpha \times T_i) + f_i^{l_a}.offset + ldelay^{l_a}) \end{aligned} \quad (25)$$

If f_i and f_j come from the same input port, l_a and l_b can be the same dataflow link.

10) *e2e delay constraints*: The e2e delay of a flow consists of 5GS and TSN parts. For the 5GS part, the delay is actually $f_i^{h_1}.span + T_{proc,gNB}$, where $T_{proc,gNB}$ is the (constant) processing delay of BS to receive packets. For TSN part, the delay is always fixed due to the AAM. It can be calculated using Eq. (2) in Section III-C. Thus, the e2e delay can be calculated by Eq. (3), and its elements that make up the formula are calculated as:

$$D_i^{5GS} = f_i^{h_1}.span + T_{proc,gNB} \quad (26)$$

$$\begin{aligned} D_{i,(1)}^{TSN} = (f_i^{l_{h_i-1}}.offset + f_i^{l_{h_i-1}}.span + ldelay^{l_{h_i-1}}) \\ - f_i^{l_2}.offset \end{aligned} \quad (27)$$

$$D_{i,(2)}^{TSN} = f_i^{h_i}.span + ldelay^{l_{h_i}}. \quad (28)$$

The e2e delay constraints can thus be described as:

$$\begin{aligned} \forall f_i \in F : \\ D_i^{e2e} \leq f_i.delay. \end{aligned} \quad (29)$$

D. Objective Function

In addition to the TT flows, many other types of flows (e.g., best-effort (BE) flows) may exist in an industrial setting. We need to reduce the resources used by TT flows and leave as much resource as possible for the BE flows.

For the 5GS part, we try to minimize the number of RBs assigned to TT flows, which is inspired by [26] (we omit the superscript l for readability as there is only one dataflow link in 5GS on the uplink):

$$\min \sum_{k \in \mathcal{F}} \frac{y_k}{|\mathcal{F}|}. \quad (30)$$

For the TSN part, as we adopt the AAM, over-provisioned transmission opportunities will lead to unused resources. Thus, in TSN, we want to maximize the periods of the transmission opportunities reserved for the flows to reduce waste of resources:

$$\max \sum_{f_i \in F} \frac{T_i}{f_i.period \cdot |F|}. \quad (31)$$

To obtain the final objective function, we multiply Eq. (31) by -1 to change the optimization direction, and then use a weighting factor γ to balance the two optimization objectives:

$$\min[\gamma \sum_{k \in \mathcal{F}} \frac{y_k}{|\mathcal{F}|} - (1 - \gamma) \sum_{f_i \in F} \frac{T_i}{f_i.period \cdot |F|}], \quad (32)$$

where $\gamma \in [0, 1]$ indicates which network we want to optimize more.

TABLE II
 TEST CASES

Flow type	Period	Size	Delay	Amount
I	0.5ms	96B	0.5ms	5
II	1ms	128B	1ms	5
III	2ms	256B	2ms	10

E. Problem Linearization

The ATSM proposed above can be transformed into an Integer Linear Programming problem. The "logical or" in Eqs. (18), (24) and (25) and the product of binary variable and bounded variable in Eqs. (16) and (17) can be linearized by the commonly used linearization methods [27]. But there still remains a difficulty: the number of constraints in Eqs. (24) and (25) cannot be determined as the number is related to the T_i and T_j which are decision variables.

To overcome this difficulty, we adopt the following strategy:

- The minimum resource period can be supported by TSN is denoted as $\min P$ whose unit is μs .
- For any flow f_i whose period is $f_i.\text{period}$, the available resource period for it can only be selected from the list $\text{list}_i = [\min P, 2 \times \min P, 4 \times \min P, \dots, T_{i,\max}]$ whose length is s_i and $T_{i,\max}$ satisfies:

$$T_{i,\max} = \min P \cdot 2^{s_i-1} \quad (33)$$

$$\min P \times 2^{s_i-1} \leq f_i.\text{period} \quad (34)$$

$$\min P \times 2^{s_i} > f_i.\text{period}. \quad (35)$$

- For any flow f_i we introduce s_i binary variables $\{b_{i,j} | j = 0, 1, \dots, s_i - 1\}$, and we let $T_i = \sum_{j=0}^{s_i-1} \text{list}_i[j] \times b_{i,j}$.

Furthermore, we introduce new constraints to make only one element of the list selected:

$$\begin{aligned} \forall f_i \in F : \\ \sum_{j=0}^{s_i-1} b_{i,j} = 1. \end{aligned} \quad (36)$$

This way, the hyper period of the set $\mathbf{T}_{\max} = \{T_{i,\max} | f_i \in F\}$ is multiple of the hyper period of the set $\mathbf{T} = \{T_i | f_i \in F\}$. Then, we can expand the check range from $[0, \frac{T_{TSN}}{T_i} - 1]$ to $[0, \frac{LCM(\mathbf{T}_{\max})}{\min P} - 1]$ in Eqs. (16) and (17).

The optimization problem is transformed into an Integer Linear Programming problem. We use Gurobi [28] to solve the problem.

V. PERFORMANCE EVALUATION

We evaluate the performance of AAM and ATSM. All simulations are conducted with the discrete-event simulator OMNET++ [16] with INET [30] and Simu5G [31] framework.

A. Simulation Setup

The topology of the simulation network is shown in Fig. 6, which has referenced the medium-sized topology in [6] and is extended with a 5GS, where blue squares represent ESs and red diamonds represent TSN switches. There are 36 ESs

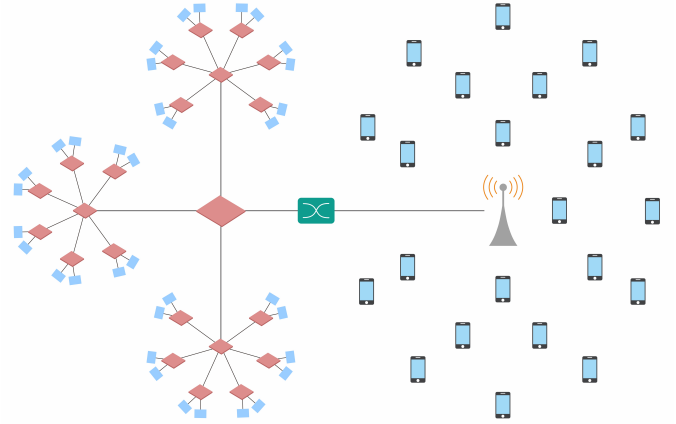


Fig. 6. Simulation network topology consisting of one 5GS and a TSN network.

 TABLE III
 SIMULATION PARAMETERS

Type	Parameter	Value
Wireless	Subcarriers spacing	120kHz
	Mini-slot duration (TTI)	7 OFDM symbols
	k_{\max}	10
	$T_{\text{proc},gNB}$	1 TTI
	Carrier Frequency	3.8 GHz
Wired	Channel Model	Urban Macrocell according to [29]
	Datarate	100 Mbps
	Propagation delay	1us
	minP	100us

in TSN and 20 UEs uniformly distributed around the base station in 5GS. There are a total of 20 flows, consisting of three types, and the specific configuration is shown in Table II, which has referenced [32]. The remaining main simulation parameters are summarized in Table III.

B. Evaluation of AAM

In the first set of experiments, we evaluate the performance of AAM compared to TAM in the presence of the 5G transmission jitter and the clock skew between the two systems. To distinguish between different experiments, we name the experiment conducted by the ATSM introduced in Section IV as the AAM-Scheduling. The baseline is called the TAM-Scheduling, which is done with a scheduling model called the *synchronous traffic scheduling model* (STSM). The STSM is modified from the ATSM by not applying the AAM, i.e., the period of the potential transmission instances equals the flow period, the packets have to arrive at the GW before the start of the transmission opportunity prepared for it, and no holding process is adopted as in [22].

As shown in Eqs. (37) and (38), we use the coefficient of expansion (CE) and coefficient of variation (CV) of the e2e delay to evaluate the ratios of e2e delay enlargement and e2e jitter, respectively, which are defined respectively as the ratio of the mean actual e2e delay to the scheduled delay and that of the standard deviation of the e2e delay to the mean actual e2e delay:

$$\forall f_i \in F :$$

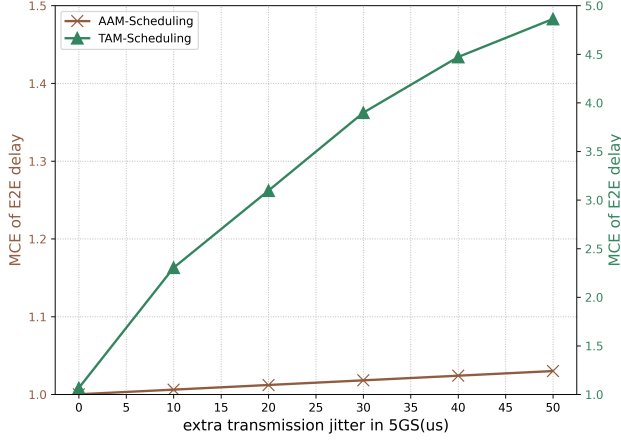


Fig. 7. The mean coefficient of expansion (MCE) of e2e delay varies with extra 5G transmission jitter.

$$CE_i = \frac{\bar{D}_{i,Actual}^{e2e}}{D_{i,Scheduled}^{e2e}} \quad (37)$$

$$CV_i = \frac{\sigma(D_i^{e2e})}{\bar{D}_{i,Actual}^{e2e}}, \quad (38)$$

where $D_{i,Scheduled}^{e2e}$ is the e2e delay calculated by the ATSM or the STSM, which both assume no transmission jitter in 5GS, $\bar{D}_{i,Actual}^{e2e}$ is the mean e2e delay the packets actually experience, and $\sigma(\cdot)$ is the standard deviation calculated by accounting for the e2e delay of each data packet.

Then, the mean coefficient of expansion (MCE) and mean coefficient of variation (MCV) are calculated to evaluate the ratios of e2e delay enlargement and jitter of the whole system:

$$MCE = \sum_{f_i \in F} \frac{CE_i}{|F|} \quad (39)$$

$$MCV = \sum_{f_i \in F} \frac{CV_i}{|F|}. \quad (40)$$

1) *Performance with 5G transmission jitter:* We first assume 5GS and TSN are synchronized and introduce an extra transmission jitter in 5GS in addition to the original 5G transmission jitter. Specifically, We vary the extra transmission jitter from $0us$ to $50us$ with step $10us$ by introducing a random extra delay in 5GS for each packet, and the extra delay follows a uniform distribution. For example, if the extra transmission jitter equals $10us$, the introduced extra delay for a packet in 5GS is sampled from the uniform distribution $U(0us, 10us)$. The results are plotted in Figs. 7, 8 and 9.

In Fig. 7, the MCE of the e2e delay of the TAM-Scheduling increases rapidly as the extra transmission jitter increases, since more packets will miss their corresponding transmission opportunities and a miss will incur an additional delay equal to the flow period as shown in Fig. 2b. However, the MCE of the AAM-Scheduling rather increases slowly compared to that of the TAM-Scheduling because a miss of transmission opportunity has no impact on the constant delay in TSN as shown in Fig. 2d and Eq. (2), and the e2e delay increases

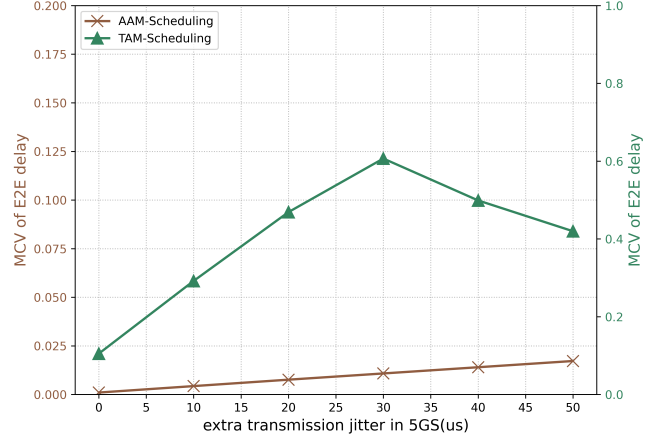


Fig. 8. The mean coefficient of variance (MCV) of e2e delay varies with extra 5G transmission jitter.

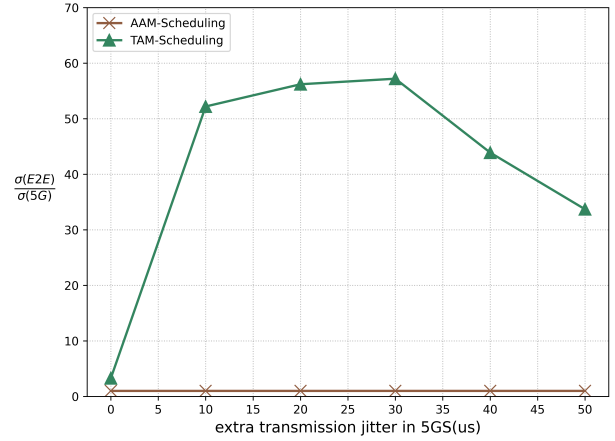


Fig. 9. The ratio of the standard deviation of e2e delay to the standard deviation of 5GS delay varies with extra 5G transmission jitter.

with the delay in 5GS which is affected by the thus-introduced mean extra transmission delay. Thus, the delay enlargement is significantly mitigated by the AAM, which is consistent with Fig. 2d.

Figs. 8 and 9 show the MCV and ratio of the standard deviation of e2e delay to the standard deviation of 5GS delay for the TAM-Scheduling and the AAM-Scheduling. In these two figures, the curves of the TAM-Scheduling first increase rapidly, because more packets will miss their transmission opportunities as the extra transmission jitter increases, and then they will decrease after the peak because more packets are transmitted in the next transmission opportunities in their next flow periods, thus decreasing the e2e jitter. However, the MCV of the AAM-scheduling increases rather slowly compared to that of the TAM-Scheduling, and the ratio of the standard deviation of the e2e delay to the standard deviation of 5GS delay is always 1 as shown in Fig. 9. This is because the transmission delay in TSN is constant and the e2e jitter is only

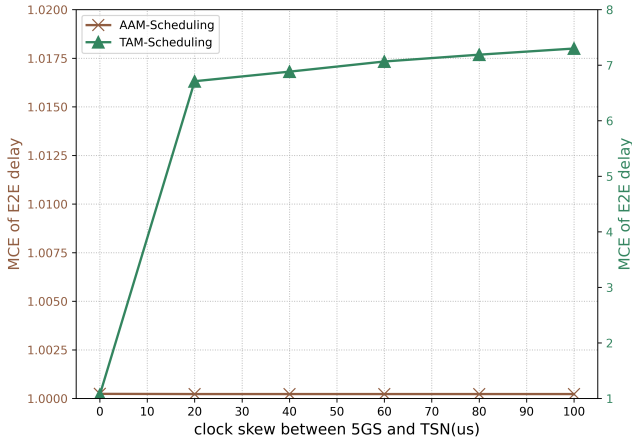


Fig. 10. The mean coefficient of expansion (MCE) of e2e delay varies with clock skew between 5GS and TSN.

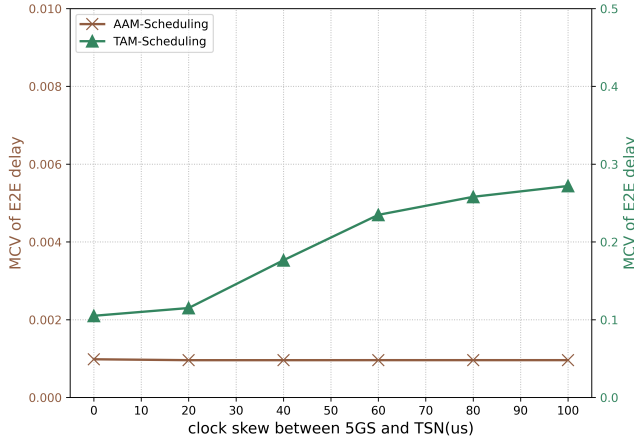


Fig. 11. The mean coefficient of variance (MCV) of e2e delay varies with clock skew between 5GS and TSN.

contributed by the 5G transmission jitter. From the above two figures, one can see that the jitter enlargement is mitigated significantly by the AAM as well.

However, the AAM provides such excellent transmission performance for TT flows at the cost of over-provisioning the transmission opportunities, wasting more resources. Even though the traffic load is the same in the two schedules, TSN resource usage by the TT flows in the AAM-Scheduling is 44.24% while the TAM-Scheduling only uses 23.04%, where TSN resource usage is defined as the ratio of the sum of the time duration when the gateway's output port is open for TT flows to the total simulation time.

2) *Performance under clock skew*: We keep the 5G transmission jitter fixed and introduce different clock skew between the two systems. Specifically, the clock skew is changed from 20us to 100us with step 20us and the clock deviation follows a uniform distribution. For example, if the clock skew equals 20us, the deviation between the clocks of TSN and 5G is

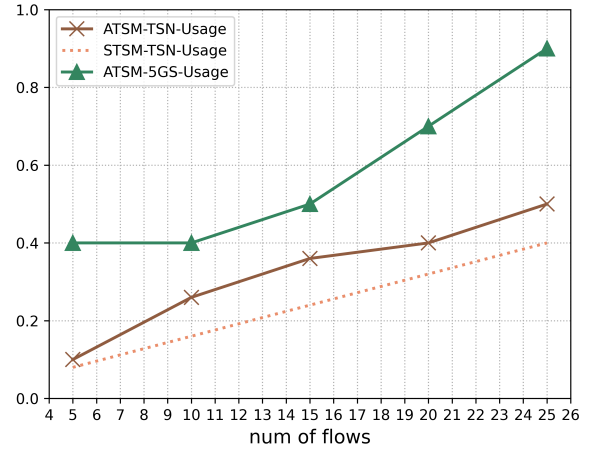


Fig. 12. TSN and 5GS resource usage scheduled by the ATSM with different numbers of flows.

sampled from the uniform distribution $U(-10us, 10us)$, and the positive values indicate that the clock of TSN is earlier than 5GS, and vice versa. The experiment results are plotted in Figs. 10 and 11.

As shown in Fig. 10, the MCE of the TAM-Scheduling increases as the clock skew increases, consistent with the situations shown in Fig. 2a. And the MCE of the AAM-Scheduling is fixed which is consistent with the situation shown in Fig. 2c. Fig. 11 shows similar results. Thus, the AAM can significantly mitigate the delay and jitter enlargement caused by the clock skew between the two systems, indicating the converged network can still work normally without time synchronization.

C. Evaluation of the ATSM

In the second set of experiments, we evaluate the performance of the ATSM in the resource assignment under different traffic loads and optimization preferences. All flows have the same parameters and the length is 200B while the period as well as the delay requirement are 1ms. We then change the number of flows to denote different traffic loads and change the γ to denote different optimization preferences.

We then calculate TSN resource usage and 5GS resource usage, where 5GS resource usage is the ratio of the RBs allocated to the TT flows to the whole number of RBs in 5GS. In addition to the two types of resource usage of the ATSM, TSN resource usage of the STSM is also computed to represent the theoretical limit of TSN resource usage that can be achieved by the ATSM.

1) *Performance under different traffic loads*: First, the number of flows is changed from 5 to 25 with step size = 5 while other parameters are fixed and $\gamma = 0.5$. The relevant results are plotted in Fig. 12.

The resource usage of both 5GS and TSN increases with the number of flows. When the traffic load is low (5 flows), TSN resource usage is the main resource bottleneck of the whole system. In order to reduce TSN resource usage, the ATSM tries

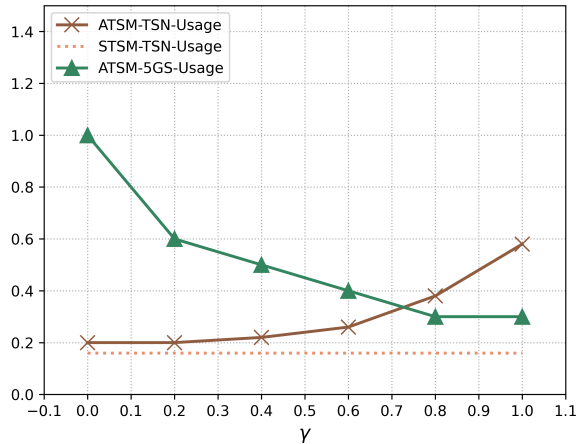


Fig. 13. TSN and 5GS resource usage scheduled by the ATSM with different γ .

to allocate larger resource periods to these flows in TSN, thus decreasing the delay budget in 5GS. To guarantee the delay in 5GS, many RBs are allocated by the ATSM, resulting in the low TSN resource usage and high 5GS resource usage. As the load increases (10 and 15 flows), wireless resource rapidly becomes scarcer. In order to reduce the use of RBs in 5GS, ATSM will arrange more flows to be sent in more TTIs and fewer RBs, where the delay budgets in 5GS increase. The model will allocate smaller resource periods to some flows in order to meet their delay requirements. Thus, the slope of TSN resource usage of the ATSM is steeper than that of the STSM. When the number reaches 20 and 25, the RBs used in 5GS cannot be reduced too much in order to meet the constraints, so ATSM will allocate larger resource periods if possible, which decreases of the steepness of the ATSM slope. TSN resource usage allocated by the ATSM is shown to be always higher than that of the STSM. The ATSM can thus keep a good balance between TSN and 5GS resource usage under different traffic loads.

2) *Performance under the different optimization preferences:* We now change the γ from 0 to 1 with step size = 0.2 and the number of flows is 10. The relevant results are plotted in Fig. 13.

The trend of the two curves is that as γ increases, the 5GS resources usage decreases while the TSN resource usage increases. When γ changes from 0 to 0.2, the 5GS resource usage experiences a sudden decrease since the ATSM start to take care of it, and an opposite phenomenon occurs to the TSN resource usage when γ changes from 0.8 to 1. Then, the two resource usages gradually increase or decrease but the absolute slope of TSN resource usage is less steeper than that of 5GS. This is because that the linearization method introduced in Section IV-E provides little room for the ATSM to optimize the TSN resource usage, so it is easier to optimize that of 5GS. The ATSM can thus use γ to apply different optimization preferences but it's easier to optimize the 5GS resource usage.

VI. CONCLUSION

To mitigate the delay and jitter enlargement when 5GS and TSN are integrated by TAM, we have presented a new mechanism, AAM, for this integration. With this mechanism, the jitter of the e2e transmission is isolated only in 5GS and packets from 5GS to TSN can be delivered at any time without time synchronization at the cost of wired bandwidth. To coordinate the allocation of resources in the converged network, we have then proposed a scheduling model called ATSM based on the AAM. Finally, the performance of the AAM and the ATSM have been corroborated via simulation using the OMNET++ simulator.

As the AAM trades resources for the ability to enable asynchronous access for traffic, in future we will consider how to dynamically utilize the allocated but un-utilized resources effectively.

REFERENCES

- [1] J. García-Morales, M. C. Lucas-Estañ, and J. Gozávez, "Latency-sensitive 5g ran slicing for industry 4.0," *IEEE Access*, vol. 7, pp. 143 139–143 159, 2019.
- [2] M. Wollschlaeger, T. Sauter, and J. Jasperneite, "The future of industrial communication: Automation networks in the era of the internet of things and industry 4.0," *IEEE Industrial Electronics Magazine*, vol. 11, pp. 17–27, 2017.
- [3] C. von Arnim, M. Dragan, F. Frick, A. Lechler, O. Riedel, and A. W. Verl, "Tsn-based converged industrial networks: Evolutionary steps and migration paths," *2020 25th IEEE International Conference on Emerging Technologies and Factory Automation (ETFA)*, vol. 1, pp. 294–301, 2020.
- [4] M. Gundall, C. Glas, and H. D. Schotten, "Feasibility study on virtual process controllers as basis for future industrial automation systems," in *2021 22nd IEEE International Conference on Industrial Technology (ICIT)*, vol. 1, 2021, pp. 1080–1087.
- [5] "Industrial ethernet is now bigger than fieldbuses," 2018. [Online]. Available: <https://www.hms-networks.com/news-and-insights/news-from-hms/2018/02/27/industrial-ethernet-is-now-bigger-than-fieldbuses>
- [6] M. L. Raagaard and P. Pop, "Optimization algorithms for the scheduling of iecce 802.1 time-sensitive networking (tsn)," 2018.
- [7] L.-M. Deng, G. Xie, H. Liu, Y. Han, R. Li, and K. Li, "A survey of real-time ethernet modeling and design methodologies: From avb to tsn," *ACM Computing Surveys (CSUR)*, vol. 55, pp. 1 – 36, 2022.
- [8] "Time-sensitive networking task group," 2023. [Online]. Available: <https://www.ieee802.org/1/pages/tsn.html>
- [9] L. L. L. Bello and W. Steiner, "A perspective on iecce time-sensitive networking for industrial communication and automation systems," *Proceedings of the IEEE*, vol. 107, pp. 1094–1120, 2019.
- [10] M. Khoshnevisan, V. Joseph, P. K. Gupta, F. Meshkati, R. Prakash, and P. Tinnakornsrisuphap, "5g industrial networks with comp for urllc and time sensitive network architecture," *IEEE Journal on Selected Areas in Communications*, vol. 37, pp. 947–959, 2019.
- [11] D. Ginthör, J. von Hoyningen-Huene, R. Guillaume, and H. D. Schotten, "Analysis of multi-user scheduling in a tsn-enabled 5g system for industrial applications," *2019 IEEE International Conference on Industrial Internet (ICII)*, pp. 190–199, 2019.
- [12] M. K. Atiq, R. Muzaffar, Ó. Seiyo, I. Val, and H.-P. Bernhard, "When iecce 802.11 and 5g meet time-sensitive networking," *IEEE Open Journal of the Industrial Electronics Society*, vol. 3, pp. 14–36, 2022.
- [13] P. Kehl, J. Ansari, M. H. Jafari, P. Becker, J. Sachs, N. König, A. Göppert, and R. H. Schmitt, "Prototype of 5g integrated with tsn for edge-controlled mobile robotics," *Electronics*, 2022.
- [14] F. Hamidi-Seppehr, M. Sajadieh, S. Panteleev, T. Islam, I. Karls, D. Chatterjee, and J. Ansari, "5g urllc: Evolution of high-performance wireless networking for industrial automation," *IEEE Communications Standards Magazine*, vol. 5, pp. 132–140, 2021.
- [15] 3GPP, "System architecture for 5g system (release 17)," 3GPP, Tech. Rep. TS 23.501, 3 2023.
- [16] "Omnet++ discrete event simulator," 2023. [Online]. Available: <https://omnetpp.org/>

[17] A. Larrañaga, M. C. Lucas-Estañ, I. Martinez, and J. Gozávez, “5g configured grant scheduling for 5g-tsn integration for the support of industry 4.0,” *2023 18th Wireless On-Demand Network Systems and Services Conference (WONS)*, pp. 72–79, 2023.

[18] Y. Cai, X. Zhang, S. Hu, and X. Wei, “Dynamic qos mapping and adaptive semi-persistent scheduling in 5g-tsn integrated networks,” *China Communications*, vol. 20, pp. 340–355, 2023.

[19] J. Yang and G. Yu, “Traffic scheduling for 5g-tsn integrated systems,” *2022 International Symposium on Wireless Communication Systems (ISWCS)*, pp. 1–6, 2022.

[20] X. Wang, H. Yao, T. Mai, S. Guo, and Y. Liu, “Reinforcement learning-based particle swarm optimization for end-to-end traffic scheduling in tsn-5g networks,” *IEEE/ACM Transactions on Networking*, 2023.

[21] “Decage: Decentralized flow scheduling for industrial 5g and tsn integrated networks,” *IEEE Transactions on Network Science and Engineering*, 2023. [Online]. Available: <https://api.semanticscholar.org/CorpusID:260800129>

[22] D. Ginhör, R. Guillaume, J. von Hoyningen-Huene, M. Schüngel, and H. D. Schotten, “End-to-end optimized joint scheduling of converged wireless and wired time-sensitive networks,” *2020 25th IEEE International Conference on Emerging Technologies and Factory Automation (ETFA)*, vol. 1, pp. 222–229, 2020.

[23] W. Steiner, “An evaluation of smt-based schedule synthesis for time-triggered multi-hop networks,” *2010 31st IEEE Real-Time Systems Symposium*, pp. 375–384, 2010.

[24] T. Zhang, J. Feng, Y. Ma, S. Qu, F. Ren *et al.*, “Survey on traffic scheduling in time-sensitive networking,” 2022.

[25] D. Jiang, H. Wang, E. M. Malkamaki, and E. Tuomaala, “Principle and performance of semi-persistent scheduling for voip in lte system,” *2007 International Conference on Wireless Communications, Networking and Mobile Computing*, pp. 2861–2864, 2007.

[26] G. Karadag, R. Gul, Y. Sadi, and S. C. Ergen, “Qos-constrained semi-persistent scheduling of machine-type communications in cellular networks,” *IEEE Transactions on Wireless Communications*, vol. 18, pp. 2737–2750, 2019.

[27] S. P. Boyd and L. Vandenberghe, “Convex optimization,” *IEEE Transactions on Automatic Control*, vol. 51, pp. 1859–1859, 2004.

[28] Gurobi Optimization, LLC, “Gurobi Optimizer Reference Manual,” 2022. [Online]. Available: <https://www.gurobi.com>

[29] 3GPP, “Study on channel model for frequencies from 0.5 to 100 ghz (release 17),” 3GPP, Tech. Rep. TR 38.901, 3 2022.

[30] “Inet framework,” 2023. [Online]. Available: <https://inet.omnetpp.org/>

[31] G. Nardini, D. Sabella, G. Stea, P. Thakkar, and A. Virdis, “Simu5g—an omnet++ library for end-to-end performance evaluation of 5g networks,” *IEEE Access*, vol. 8, pp. 181 176–181 191, 2020.

[32] I. I. Consortium *et al.*, “Time sensitive networks for flexible manufacturing testbed characterization and mapping of converged traffic types,” 2019.



Chunxi Li received the B.S. degree in telecommunication engineering, and the M.S. and Ph.D. degrees in communication and information systems from Beijing Jiaotong University (BJTU), Beijing, China, in 1992, 1997, and 2010, respectively.

He is currently an Associate Professor with the School of Electronic and Information Engineering, BJTU. His research interests include measurement and modeling on online mobile streaming systems, distributed caching network, and industrial traffic scheduling.



Zonghui Li received the B.S. degree in computer science from the Beijing Information Science and Technology University in 2010, and the M.S. and Ph.D. degree from the Institute of Microelectronics and the School of Software, Tsinghua University, Beijing, China, in 2014 and 2019, respectively.

He is currently an associate professor in the School of Computer and Information Technology, Beijing Jiaotong University, Beijing, China. His research interests include embedded and high performance computing, real-time embedded systems,

especially for industrial control networks and fog computing.



Kang G Shin (Life Fellow, IEEE) received the BS degree in electronics engineering from Seoul National University, Seoul, Korea, and the MS and PhD degrees in electrical engineering from Cornell University, Ithaca, New York, in 1970, 1976, and 1978, respectively. He is the Kevin & Nancy O’Connor Professor of Computer Science in the Department of Electrical Engineering and Computer Science, The University of Michigan, Ann Arbor. His current research focuses on QoS-sensitive computing and networking as well as on embedded real-time and

cyber-physical systems.

He has supervised the completion of 91 PhDs, and authored/coauthored close to 1,000 technical articles, a textbook and about 60 patents or invention disclosures, and received numerous awards, including the 2022 IEEE Computer Society Technical & Conference Activities Board Distinguished Leadership Award in real-time systems. He is also an ACM Fellow.



Jiacheng Li received the B.S. degree in telecommunication engineering from the School of Electronic and Information Engineering, Beijing Jiaotong University (BJTU), Beijing, China, in 2021, where he is currently pursuing his M.S. degree.

His research interests include industrial real-time networking and traffic scheduling.



Yongxiang Zhao received the Ph.D. degree in electrical engineering from BJTU, Beijing, China, in 2002.

He is currently an Associate Professor with the School of Electronic and Information Engineering, BJTU. His research interests include network protocol and algorithm design, quality of video streaming, and modeling and design of communication networks.



Bo Ai (Fellow, IEEE) received his Master degree and Ph. D. degree from Xidian University in China. He graduated from Tsinghua University with the honor of Excellent Postdoctoral Research Fellow in 2007. He was a visiting professor at EE Department, Stanford University in 2015. He is now working at Beijing Jiaotong University as a full professor and Ph. D. candidate advisor. He is the Deputy Director of State Key Lab of Rail Traffic Control and Safety, and the Deputy Director of International Joint Research Center.

He has authored/co-authored 8 books and published over 300 academic research papers in his research area. He has hold 26 invention patents. He is a Fellow of the Institution of Engineering and Technology (IET Fellow), IEEE VTS Distinguished Lecturer. He has received many awards including Distinguished Youth Foundation and Excellent Youth Foundation from National Natural Science Foundation of China.